Regulatory T cells increase the avidity of primary CD8+ T cell responses and promote memory

Luigia Pace 1, Andy Tempez 1*, Catharina Arnold-Schrauf 2*, Fabrice Lemaitre 3, Philippe Bousso 3, Luc Fetler 4§, Tim Sparwasser 2§ and Sebastian Amigorena 1

*1 INSERM U932, Institut Curie, Immunity and Cancer, F-75248 Paris, France*

2 *Institute of Infection Immunology, TWINCORE, Centre for Experimental and Clinical Infection Research, 30625, Hannover, Germany*.

*3 INSERM U668, Institut Pasteur, Department of Immunology, F-75015, Paris, France*

*4 CNRS UMR 168, Laboratoire de Physico- Chimie Curie, Institut Curie, F-75248 Paris Cedex 05, France*

**§ Contributed equally to this work*

*Corresponding author: sebastian.amigorena@curie.fr*

Although regulatory T cells (Tregs) are known to suppress self-reactive autoimmune responses, their role during T cell responses to non-self antigens is not well understood. We show that Tregs play a critical role during the priming of immune responses in mice. Treg depletion induced the activation and expansion of a population of low avidity CD8+ T cells due to over production of CCL-3/4/5 chemokines, which stabilized the interactions between antigen presenting dendritic cells and low avidity T cells. In the absence of Tregs, the avidity of the primary immune response was impaired, resulting in reduced memory to *Listeria monocytogenes*. These results suggest that Tregs are important regulators of the homeostasis of CD8+ T cell priming and play a critical role in the induction of high avidity primary responses and effective memory.

In the absence of Foxp3+ regulatory T cells (Tregs), fatal multiple organ autoimmune pathologies arise, leading to death in both human and mice (*1*). Tregs suppress autoreactive T cells through multiple effector mechanisms, acting both during priming in lymph nodes and during the effector phases of immune and inflammatory responses (*1-5*). In healthy individuals, intriguingly, Treg-mediated suppression does not compromise T cell responses to infectious, non-self antigens. Previous reports propose that Tregs not only inhibit immune responses to non-self antigens, but also may contribute to clearance of viral or parasite infections (*6, 7*). How Tregs contribute to priming of T lymphocytes to non-self antigens remains unclear.

To investigate the role of Tregs in CD8+ T cell responses to non-self antigens, we used mice expressing the human diphtheria toxin receptor (DTR) under the control of the Foxp3 promoter (DEREG mice). After two diphtheria toxin (DT) injections (*8*) we confirmed Treg depletion and the absence of any detectable polyclonal T cell activation or changes in DC number and activation (*9*).

We first analyzed the response to the H-Y male-specific histocompatibility antigen Uty in female mice. We immunized Treg-depleted or control female mice with male splenocytes, and measured the response against an Uty-peptide by using $D^b$-Uty multimers. Immunization of control females induced a uniform population of CD8+ T cells strongly labeled by the multimer (Fig. 1A). Depletion of Tregs during priming (subgroup G1, received DT on days -1, 0, 5, and 6, fig. S1A), resulted in the expansion in all mice analyzed (n=20) of a distinct population of CD8+ T cells that bound low amounts of multimers, accompanied by an increase in the total numbers of multimer positive cells (Fig. 1A-C). The expression of CD8 was not modified (fig. S1B). In

some Treg-depleted mice, the high multimer binding CD8+ T population disappeared, most likely due to competition or to differences in the T cell receptor (TCR)-repertoires. The intensity of multimer binding reflects the affinity of the TCR for major histocompatability complex (MHC)-peptide complexes (*10-15*). The ratio between the mean fluorescent intensity (MFI) for multimer to the MFI for TCR expression (relative affinity) was decreased in the absence of Tregs, as compared to control littermates (Fig. 1D, fig. S1C). A better estimate of the avidity of the polyclonal response can be obtained using a multimer dilution assay (*12, 15, 16*), where the avidity of the response is estimated using the EC50. The $D^b$-Uty multimer dilution assay showed a clear decrease in the avidity of the anti-Uty response upon depletion of Tregs (Fig. 1E-F, fig. S1D).

To investigate whether the impact of Tregs on CD8+ T cell avidity operates during the early phases of T cell activation (i.e. priming) or later during T cell expansion, we delayed the depletion of Tregs (G2: DT on days 3, 4, 9, 10; G3: DT on days 5, 6 and 11, fig. S1A). Delayed Treg-depletion still caused an increase in the percentage of Db-Uty+ T cells, indicating that in all cases Tregs limit T cell expansion (fig. S2A). Decreased T cell avidity, by contrast, was only observed when the depletion of Tregs was performed during priming (fig. S2B-D). We conclude that the presence of Tregs during T cell priming to a non-self antigen increases the affinity of the CD8+ T cell response, most likely by inhibiting the priming of T cells bearing low avidity antigen-specific TCRs.

To generalize this observation to other antigens, we next analyzed a CD8+ T cell response to the OVA peptide 257-264 (SIINFEKL, N4) after immunization with peptide loaded LPS-treated

DCs and obtained similar results (fig. S3, A-D). In spite of the increase in total $K^b$-N4 multimer-positive cells after priming in Treg-depleted mice (fig. S3B), the number or relative affinity of antigen-specific CD8+ memory T cells after challenge (which is increased as compared to the avidity of the primary cells) was not enhanced in DEREG mice deprived of Tregs during priming (fig. S3B and D). Indeed, the ratio between the mean number of memory and primary multimer-positive cells was decreased upon Treg depletion during priming (fig. S3C), indicating that the numerous low avidity OVA-specific T cells that proliferate in the absence of Tregs do not give rise to long-lived memory cells.

Because Treg depletion can perturb the environment, which could indirectly affect T cell priming, we decided to test if injection of isolated antigen-specific Tregs would increase the avidity of a polyclonal T cell response. We isolated Dby-specific, Foxp3- EGFP- T helper cells (Th) or Foxp3+ EGFP+ Tregs from Foxp3-EGFP $CD4^+$ TCR-transgenic Marilyn mice. We injected these cells into wildtype hosts previously immunized with (N4+Dby)-loaded DCs. The total numbers of $K^b$-$N4^+$ $CD8^+$ T cells were decreased when the mice were injected with Marilyn Tregs (fig. S3, E and F). Moreover, the presence of Marilyn Tregs reduced the number of low-multimer binding T cells, as compared to Marilyn Th cells, resulting in an increase in the relative affinity of the response (fig. S3, E, G and H). We concluded that the adoptive transfer of antigen-specific Tregs preferentially inhibits low avidity as opposed to high avidity CD8+ T cells, thereby increasing the overall avidity of the T cell response.

To directly test whether Tregs preferentially inhibit the priming of low avidity CD8+ T cells, we used two altered peptide ligands that are recognized with different affinities by the OT-I TCR

(OT-I is a CD8+, TCR transgenic line specific for the H-2K$^b$-SIINFEKL (N4, OVA peptide)). K$^b$-N4 complexes bind the OT-I TCR with high affinity. SIITFEKL (T4), binds K$^b$ with an affinity similar to N4, but the K$^b$-T4 complexes are recognized by the OT-I TCR with an affinity 70.7-fold lower than K$^b$-N4 complexes (*16*-*18*). We first verified that the numbers of K$^b$-N4 and K$^b$-T4 complexes present on the DC surface were similar (fig. S4, A and B). Immunization with N4-loaded DCs (N4-DCs) induced effective OT-I expansion both in the presence and absence of Tregs, although Treg depletion increased the expansion at low peptide concentrations (Fig 2A; fig. S4, C and D). T4-loaded DCs, as shown previously (*18*), induced very low expansion of OT-I cells in the presence of Tregs, even at high peptide concentrations (Fig. 2B, fig. S4, C and D). In Treg depleted mice, by contrast, T4-DCs induced effective expansion of OT-I cells over a wide range of peptide concentrations (Fig 2B). Similar results were obtained when OT-I activation was assayed using CD69 expression (Fig. S5A), suggesting that Tregs inhibit some early steps of T cell priming by low affinity peptides.

To test if Tregs suppress priming by low affinity peptide by acting directly on CD8+ T cell, we next reconstituted the inhibition *in vitro*. Tregs, but not CD4+ Th cells, inhibited the activation of OT-I cells by N4-DCs only at low peptide concentration (fig. S5B). In the case of T4-loaded DCs, the inhibition by Tregs was more potent and was observed at both high and low peptide concentrations (fig. S5C**)**. These results suggest that the expansion of low avidity polyclonal T cells observed in DEREG mice is due to the release of the suppression by Tregs of low avidity T cell clones.

Tregs were previously shown to regulate DC-T cell interactions during priming (*3, 5*) and to suppress the production by DCs of CCL-3/4 (*19, 20*), a family of chemokines involved in the control of the dynamics of T cell priming (*21-23*) as well as in the stability and signaling at DC-T cell synapse (*24, 25*). We therefore hypothesized that Tregs destabilize low avidity DC-T cell interactions more efficiently than high avidity interactions through the regulation of chemokine production.

To investigate this possibility, we first analyzed the production of CCL-3/4/5 during T cell priming *in vivo* by DCs loaded with N4 or T4 peptides, in the presence or absence of Tregs (fig. S6, A-C). In littermates, unloaded LPS-treated DCs induced the production of all three chemokines in draining popliteal lymph nodes (dpLNs). Loading of the DCs with T4 hardly modified chemokine production, whereas loading with N4 increased the production of CCL-3/4 (fig. S6, A and B). Treg-depletion did not modify the expression of activation markers by the adoptively transferred DCs (fig. S5, D-H). By contrast, it increased CCL-3/4 production in mice injected with unloaded or T4-loaded DCs, but not with N4-DCs (most likely because the production of these chemokines was already very high).

We therefore investigated the effects of Treg depletion and the eventual role of these chemokines, on DC-T cell interactions induced by high or low affinity peptides using intravital dynamic 2-photon microscopy (TPLSM). Littermates or DEREG mice treated with DT were adoptively transferred with a 1:1 mix of DsRED-expressing DCs pulsed with either N4 or T4 and unloaded control CFP+ DCs (as a control contact quantifications). GFP+ OT-I T cells were then

adoptively transferred to the mice. The possible involvement of CCL-3/4/5 was addressed using a previously described mix of blocking antibodies (*21, 23*).

The injection of blocking antibodies had no major effect on DC and OT-I recruitment to the dpLNs, as compared to control mice (fig. S7, A and B). In these mice, N4-DCs caused a marked arrest of OT-I cells, and long lasting DC-T cell contacts, as compared to T4-DCs (Movie 2 and 4, Fig. 2C-H), confirming that high affinity peptides induces longer lasting DC-T cell contacts with naïve T cells than low affinity peptides (*16, 26*). Depletion of Tregs did not affect the arrests and long lasting DC-T cell contacts observed with N4-DCs (fig. S7C). By contrast, the intermediate OT-I mean velocity (Vmean) observed in mice injected with T4-DCs was reduced upon depletion of Tregs (Fig 2C-D, G-H, movie 4 and 6), while the average contact duration of the individual contacts was increased (Fig. 2E-H) (*27*). Therefore, the low affinity T4 peptide mediates relatively stable DC-OT-I interaction only in the absence of Tregs, consistent with the observation that it only induces expansion after Treg depletion.

Treatment of the mice with CCL-3/4/5 blocking antibodies had no major effect on OT-I displacement or contact durations in the case of N4-DCs (movie 1 and Fig. 2D-F). In mice injected with T4-DCs, by contrast, the blocking antibodies reversed the effects of Treg depletion, both in terms of reduction of the Vmean and of the duration of the individual contacts (Fig. 2D-E, G-H, movie 3 and 5). The lack of effect of the chemokine antibodies in mice injected with N4-DCs could be due to the higher levels of chemokine production observed in these mice (fig. S6, A-C) or stable N4-DC-T cell conjugates may become chemokine-independent. These results suggest that the stable interactions of T cells with DCs bearing low affinity peptides that occur in

the absence of Tregs require CCL-3/4/5. We propose that by limiting the production of CCL-3/4/5, Tregs normally inhibit stable interactions between DCs and low avidity T cells, thereby limiting their priming.

To investigate the role of Tregs during CD8+ T cell responses to a microbe-associated non-self antigen, we infected DT-treated DEREG mice or littermates with *Listeria monocytogenes* expressing recombinant OVA (rLM-OVA) (*28*). Treg depletion affected neither the proportion of myeloid cells (fig. S8, A-F), nor the bacterial burden at days 3 and 5 post-infection, or the capacity of the mice to clear the infection (Fig. 3A) (clearance of the primary LM infection is known to be mainly mediated by innate immunity (*29*)). Treg depletion caused a reduction in the total numbers of $K^b$-N4 multimer-positive T cells at day 7 (peak of the response, Fig 3B). In the presence of Tregs, rLM-OVA infection induced primarily a population of high multimer-binding T cells (Fig 3C). Upon Treg depletion, the proportion of low multimer binding cells increased (Fig. 3, C and D, and fig. S9, A-D). These cells were antigen specific, as they did not bind a control $K^b$-SSIEFARL multimers (fig. S9A). Although the total numbers of both high and low multimer-binding cells decreased slightly in Treg-depleted mice, the decrease was significantly greater for the high multimer binding cells (Fig. 3D). This decrease could be due to overstimulation of high avidity T cells (which may impair T cell activation (*30*)), or to competition of the OVA-specific cells with the very numerous T cells that respond to other LM antigens in the absence of Tregs (fig. S10, A and B).

As expected from the changes in the proportions of high and low multimer-binding cells, Treg depletion induced a decrease in the relative affinity of the OVA-specific responding T cells (Fig.

3E, fig. S9, C and D). Decreased multimer labeling was not due to lower levels of CD8 expression (fig. S9B). Decrease in the avidity of the OVA-specific CD8+ T cell response upon depletion of Tregs was also evident in the multimer dilution assay (Fig. 3F and G). Interferon-**γ** (IFN**γ**) production by CD8+ T cells was shown previously to correlate with the avidity of anti-LM immune responses (*10*). Both the number of OVA-specific IFN**γ**-producing CD8+ T cells and the amount of IFN**γ**/cell (MFI) were lower when the infection took place in the absence of Tregs (fig S11, A-C). When Treg depletion was delayed to days 3-4 after infection, the relative affinity and the EC50 of multimer binding assay (Fig. 3E and G), as well as the numbers of multimer+ and IFN**γ**+ cells were all unaffected, while the MFI of the IFN**γ** labeling was slightly increased (fig. S12, A-C).

In order to investigate the mechanisms involved in the beneficial effects of Tregs during priming to LM antigens, we harvested the spleens of mice infected in the presence or absence of Tregs and analyzed different inflammatory mediators. No major effects on the secretion of CXCL1 and CXCL10, fig. S13, A-B). By contrast, the production of CCL-2/3/4 was increased upon Treg depletion *in vivo* (fig S13, C-E). Furthermore, upon *ex vivo* re-stimulation with heat killed (HK)-rLM-OVA the splenocytes isolated from infected mice showed significantly enhanced secretion of CCL-3/4/5 when the infection *in vivo* took place in the absence of Tregs (fig. S14). These findings indicate that, as shown previously by others (*19, 20*), Tregs inhibit in vivo the production of CCL-2/3/4/5.

Because our previous results implicate CCL-3/4/5 in the control of the priming of low avidity T cells, we decided to explore the possible involvement of the overproduction of these chemokines

in the detrimental effects of Treg-depletion on T cell priming during LM infection. To do so, we injected a mix of blocking antibodies to CCL-3/4/5 following Treg-depletion and infection with rLM-OVA (*21, 23*). In both isotype control and blocking antibody-treated mice, the bacteria were undetectable in the spleen at day 7. By contrast, only injection of the blocking antibodies reversed the effects of Treg-deprivation on the proportion of low and high multimer binding cells and of the relative affinity of the responding OVA-specific T cells (fig. S15, A and B). These results suggest that CCL-3/4/5 production in the absence of Tregs is required for the observed reduction in avidity of the OVA-specific CD8+ T cells after LM infection.

We next investigated the functional relevance of the presence of Tregs during the primary infection by rLM-OVA. Because the avidity of primary responses was suggested to influence memory responses (*12, 15*), we investigated the memory responses generated after LM infection in Treg-deprived mice. Littermates and DEREG mice treated with DT were primed with rLM-OVA and tested for memory responses by re-infecting the mice with rLM-OVA 50 days later. After secondary infection, 10-25 fold higher bacteria burden was detected in both spleen and liver when Tregs had been depleted before the primary infection (Fig. 4A). Consistent with this result, both the number of memory $K^b$-N4 multimer-positive T cells (Fig. 4B and C) and their relative affinity (Fig. 4D) were reduced. After *ex vivo* re-stimulation, we found reduced numbers of IFN**γ**-granzyme B double positive memory cells (Fig. 4E and F). Therefore, the presence of Tregs during the primary rLM-OVA infection is required for the establishment of fully effective high avidity CD8+ T cell memory responses.

We propose that the absence of Tregs reduces the "fitness" of primary CD8+ T cell responses, causing the over proliferation of low avidity T cells, and perhaps impairs the activation of high avidity T cells, although this remains to be explored. The inhibition of low avidity T cell clones by Tregs could also help explain why Tregs fully control T cell reactivity to self-antigens (which are generally of low avidity due to negative selection (*10*), while sparing T cell responses to non-self antigens (which target a non-negatively selected repertoire that includes high avidity T cells). These results unravel an unexpected function for Tregs during CD8+ T cell priming and should inform Treg manipulation for the design of long-term vaccination.

## FIGURE LEGENDS

**Figure 1.** Treg depletion impairs the affinity of anti-H-Y CD8+ T cell responses during naive T cell priming. **A.** Flow cytometric analysis of Uty-specific CD8+ T cells in the spleen of female littermates and DEREG mice immunized with 5x106 male splenocytes that received DT injections on days -1, 0, 5 and 6. Primary CD8+ T cell responses were measured by $D^b$-Uty multimer staining 12 days after immunization. **A.** Representative CD8+-gated plots are shown. **B.** Frequency of $D^b$-Uty multimer positive among CD8+ T cells in the spleen. L: littermante; D: DEREG. **C**. The numbers of high affinity and low affinity antigen-specific cells were determined by $D^b$-Uty multimer staining. **D**. The relative affinity (multimer/TCR MFI ratio) of $D^b$-Uty-specific CD8+ T cells. **E.** Direct *ex vivo* multimer-dilution assay. The percentage of $D^b$-Uty multimer positive cells are normalized to the number of $D^b$-Uty multimer-positive cells at the highest multimer concentration; individual mice (black line) and the mean value for each group (red line) are represented. **F.** For each mouse, the data obtained in panel E were analyzed to fit to sigmoid dose-response curves and the EC50 value for half-maximum response concentration was calculated. Results from at least 3 independent experiments are shown.

**Figure 2.** Treg suppression inhibits T cell responses to low affinity ligands by destabilizing T cell-DC interactions. **A-B**. DEREG (black) or control (white) littermates mice were DT-injected and immunized by footpad (f.p.) injection with mature DCs loaded with the indicated concentrations of the native N4 or the alternate peptide ligand T4. Eighteen hours later, mice were injected intravenously with $10^5$ naïve CD45.1 OT-I cells. OT-I cell numbers from the harvested dpLNs 5 days after the immunization is reported. **C-H**. TPSLM analysis of OT-I cell priming in DT-treated littermate and DEREG mice. DsRED+ DCs loaded or not with 1 µM of

N4 or T4 peptides and unpulsed CFP+ DCs were co-injected in the f.p. of DT-treated littermate or DEREG mice in the presence of blocking antibodies against CCL3/4/5 or the isotype-matched control antibodies. Twenty hours later, GFP+ OT-I cells were adoptively transferred. Before *in vivo* imaging, mice received the anti-L-selectin antibody to block lymphocyte homing, and dpLNs were collected 2-6 hours after OT-I cell transfer. **C**. Representative TPLSM images are shown. White lines represent migratory paths of OT-I cells. **D**. T cell mean velocities are represented, the red line indicates the median value. **E.** Average contact duration. **F-H.** The percentage of remaining conjugates for interactions between GFP+ OT-I cells and DsRED+ DCs are shown. Data are representative of at least three independent experiments. Error bars represent mean ± sem.

**Figure 3.** Tregs promote high avidity CD8+ T cell primary immune responses to rLM-OVA infection. DT-treated DEREG and littermate mice were injected i.v. with $5x10^3$ rLM-OVA. **A.** At day 3 5 and 7 after infection, the number of live bacteria per spleen (left panel) and liver (right panel) was determined. **B.** Primary CD8+ T cell responses were measured after the infection by $K^b$-N4 multimer staining. The number of CD8+ $K^b$-N4+ cells is reported. **C.** CD8+-gated flow cytometry plots from samples collected day 7 after infection are shown. **D**. The numbers of high affinity and low affinity antigen-specific cells were determined by $K^b$-N4 multimer staining. **E**. Relative affinity for $K^b$-N4+ cells was determined after early (DT day -1, 0) or late depletion (DT day 3-4). **F**. E*x vivo* multimer-dilution assay at day 7 after rLM-OVA infection. The graph shows the percentage of $K^b$-N4 multimer-positive on gated CD8+ T cells, normalized to the number of $K^b$-N4 multimer-positive cells at the highest multimer concentration. Individual mice (black line) and the mean values (red line) are represented. **G**. For

each individual mouse, the data obtained in panel F were analyzed to fit to sigmoid dose-response curves and the EC50 value for half-maximum response concentration was calculated. Treg cells were depleted at day -1 and 0 (early depletion) or at day 3 and 4 post-infection (late depletion). Error bars represent mean ± sem. Data are representative of three independent experiments.

**Figure 4.** During T cell priming Tregs are required to generate a protective immune response after secondary rLM-OVA challenge. Littermates and DEREG mice were treated with DT and infected with rLM-OVA, and tested for memory protection 50 days later. For memory T cell generation, naïve and 50-days post-infection mice were given $5x10^3$ and $2x10^5$ rLM-OVA, respectively. **A.** The number of live bacteria per spleen (left panel) and liver (right panel) was determined 3 days after secondary challenge. As control, C57BL/6 mice that had not received primary infection cells were similarly infected. In 10 over 12 spleens from littermate mice, the bacteria were undetectable. **B-F.** $K^b$- N4+ multimer and intracellular IFN**γ** and granzyme B staining were done to determine the percentage of antigen specific cells in CD8+ T cell population. **B.** CD8+-gated flow cytometry plots are shown (samples were collected 3 days after challenge). **C**. The number of H2-$K^b$-N4+ cells is shown. Individual mice are represented, control uninfected (grey), littermate (white) and DEREG (black). Results from 3 independent experiments are shown. **D**. Relative affinity for $K^b$-N4+ cells was determined. **E-F**. Following *ex vivo* N4 re-stimulation, IFN**γ** and granzyme B staining was done to determine the number of CD8+ antigen-specific cells. **E.** CD8+-gated flow cytometry plots are shown. **F.** The number of IFN**γ**+granzyme B+ CD8+ cells is shown. Data are representative of three independent experiments. Error bars represent mean ± sem.

## References


1. K. Wing, S. Sakaguchi, *Nat Immunol* **11**, 7 (Jan 2010, 2009).
2. M. Feuerer, Y. Shen, D. R. Littman, C. Benoist, D. Mathis, *Immunity* **31**, 654 (Oct 16, 2009).
3. Q. Tang *et al.*, *Nat Immunol* **7**, 83 (Jan, 2006).
4. D. R. Littman, A. Y. Rudensky, *Cell* **140**, 845 (Mar 19, 2010).
5. C. E. Tadokoro *et al.*, *J Exp Med* **203**, 505 (Mar 20, 2006).
6. Y. Belkaid, C. A. Piccirillo, S. Mendez, E. M. Shevach, D. L. Sacks, *Nature* **420**, 502 (Dec 5, 2002).
7. J. M. Lund, L. Hsing, T. T. Pham, A. Y. Rudensky, *Science* **320**, 1220 (May 30, 2008).
8. K. Lahl *et al.*, *J Exp Med* **204**, 57 (Jan 22, 2007).
9. A. Boissonnas *et al.*, *Immunity* **32**, 266 (Feb 26, 2010).
10. D. Zehn, M. J. Bevan, *Immunity* **25**, 261 (Aug, 2006).
11. E. S. Huseby *et al.*, *Cell* **122**, 247 (Jul 29, 2005).
12. D. H. Busch, E. G. Pamer, *J Exp Med* **189**, 701 (Feb 15, 1999).
13. C. Bouneaud, P. Kourilsky, P. Bousso, *Immunity* **13**, 829 (Dec, 2000).
14. M. M. Davis, J. D. Altman, E. W. Newell, *Nat Rev Immunol* **11**, 551 (2011).
15. P. A. Savage, J. J. Boniface, M. M. Davis, *Immunity* **10**, 485 (Apr, 1999).
16. H. D. Moreau *et al.*, *Immunity*, (Jun 7, 2012).
17. S. C. Jameson, M. J. Bevan, *Eur J Immunol* **22**, 2663 (Oct, 1992).
18. D. Zehn, S. Y. Lee, M. J. Bevan, *Nature* **458**, 211 (Mar 12, 2009).
19. S. Morlacchi *et al.*, *J Immunol* **186**, 6807 (Jun 15, 2011).
20. V. Dal Secco *et al.*, *PLoS One* **4**, e7696 (2009).
21. F. Castellino *et al.*, *Nature* **440**, 890 (Apr 13, 2006).
22. S. Hugues *et al.*, *Nat Immunol* **8**, 921 (Sep, 2007).
23. H. D. Hickman *et al.*, *J Exp Med* **208**, 2511 (Nov 21, 2011).
24. B. Molon *et al.*, *Nat Immunol* **6**, 465 (May, 2005).
25. R. L. Contento *et al.*, *Proc Natl Acad Sci U S A* **105**, 10101 (Jul 22, 2008).
26. R. A. Gottschalk *et al.*, *Proc Natl Acad Sci U S A* **109**, 881 (Jan 17, 2012).
27. J. B. Beltman, S. E. Henrickson, U. H. von Andrian, R. J. de Boer, A. F. Maree, *J Immunol Methods* **347**, 54 (Aug 15, 2009).
28. K. E. Foulds *et al.*, *J Immunol* **168**, 1528 (Feb 15, 2002).
29. E. G. Pamer, *Nat Rev Immunol* **4**, 812 (Oct, 2004).
30. A. M. Kalergis *et al.*, *Nat Immunol* **2**, 229 (Mar, 2001).
31. Y. Wang *et al.*, *J Immunol* **180**, 1565 (Feb 1, 2008).
32. O. Lantz, I. Grandjean, P. Matzinger, J. P. Di Santo, *Nat Immunol* **1**, 54 (Jul, 2000).
33. C. Winzler *et al.*, *J Exp Med* **185**, 317 (Jan 20, 1997).
34. C. Kervrann, J. Boulanger, *IEEE Trans Image Process* **15**, 2866 (Oct, 2006).
35. J. Boulanger *et al.*, *IEEE Trans Med Imaging* **29**, 442 (Feb, 2009).

**ACKNOWLEDGEMENTS**

We would like to thank all the U932 and Twincore Sparwasser members, D. Raulet, A. Dielmann, P. Paul-Gilloteaux, O. Lantz, M. Albert and the Nikon center platform, the animal facilities of Institut Curie and Twincore, for help with the experiments and helpful discussions. rLM-OVA was kindly provided by Prof. Hao Shen. This work was supported by funding from the Institut Curie; Institut National de la Santé et de la Recherche Médicale; Centre National de la Recherche Scientifique; La Ligue Contre le Cancer; Association de Recherche Contre le Cancer (ARC); EC grant ENCITE, Health-F5-2008-201842, SFB 900. P.L. has been supported by ARC, A.T. was a fellow of Ministère de l'Education et de la Recherche. C.A.S. was supported by the Boehringer Ingelheim Fonds, Foundation for Basic Research in Medicine. The authors have no conflicting financial interests. The data are tabulated in the main paper and in the supplementary materials.

**Figure 1 Pace L. et al.**

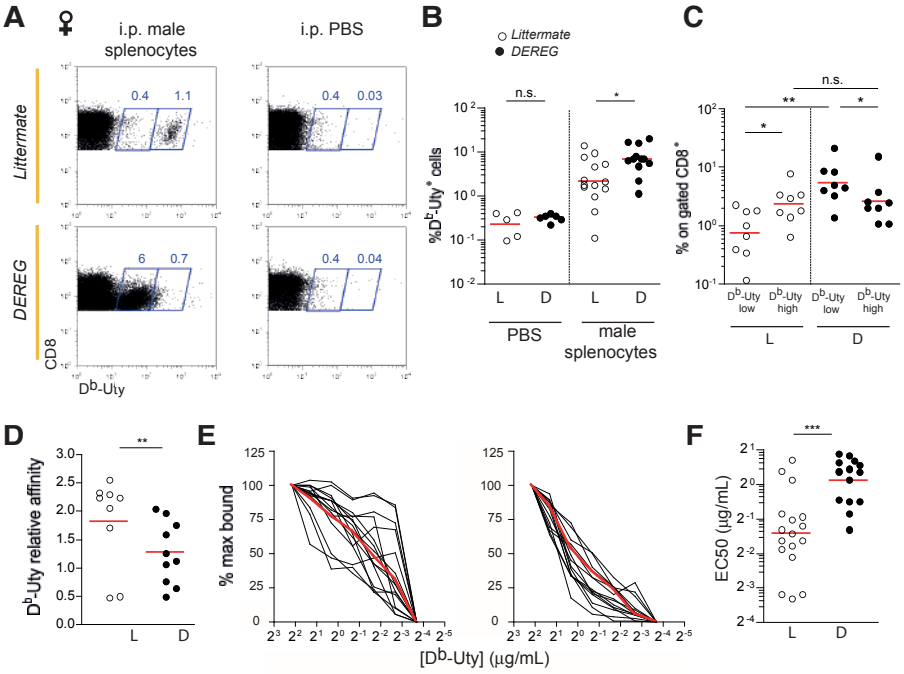

**Figure 2 Pace L. et al.**

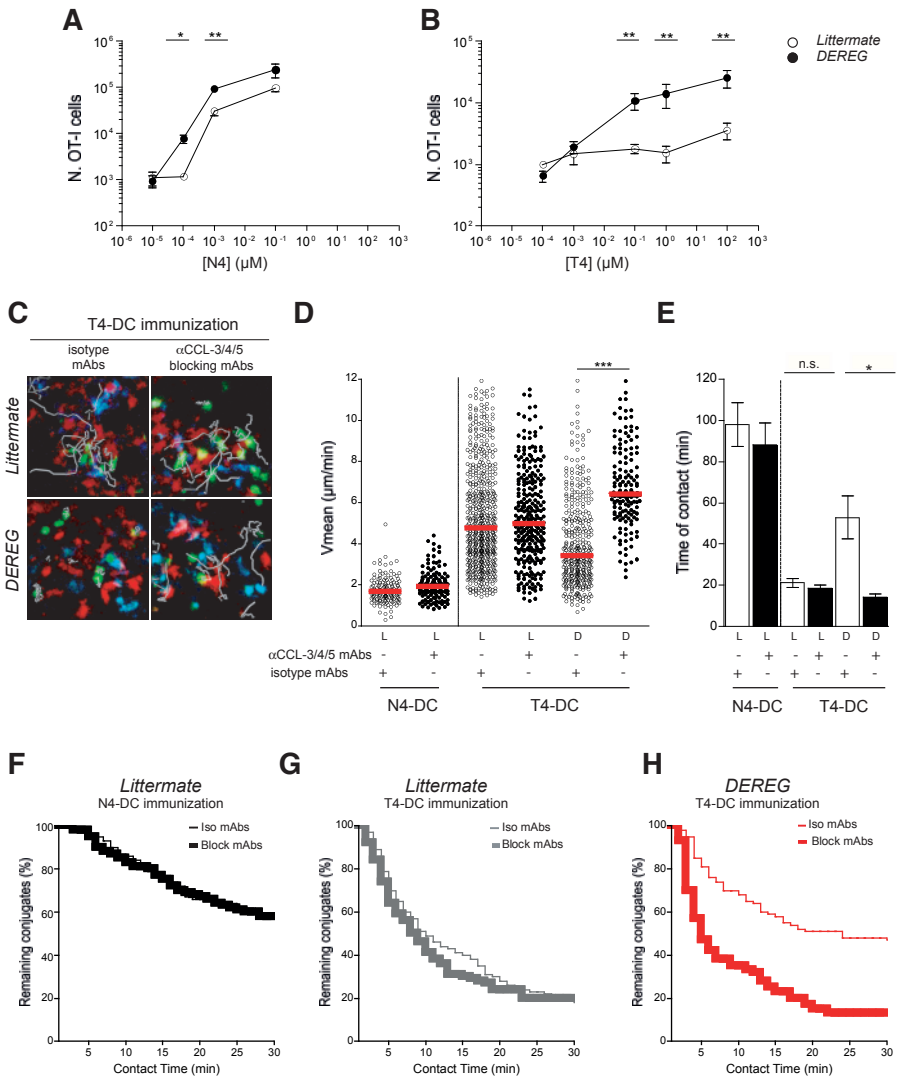

# Figure 3 Pace L. et. al.

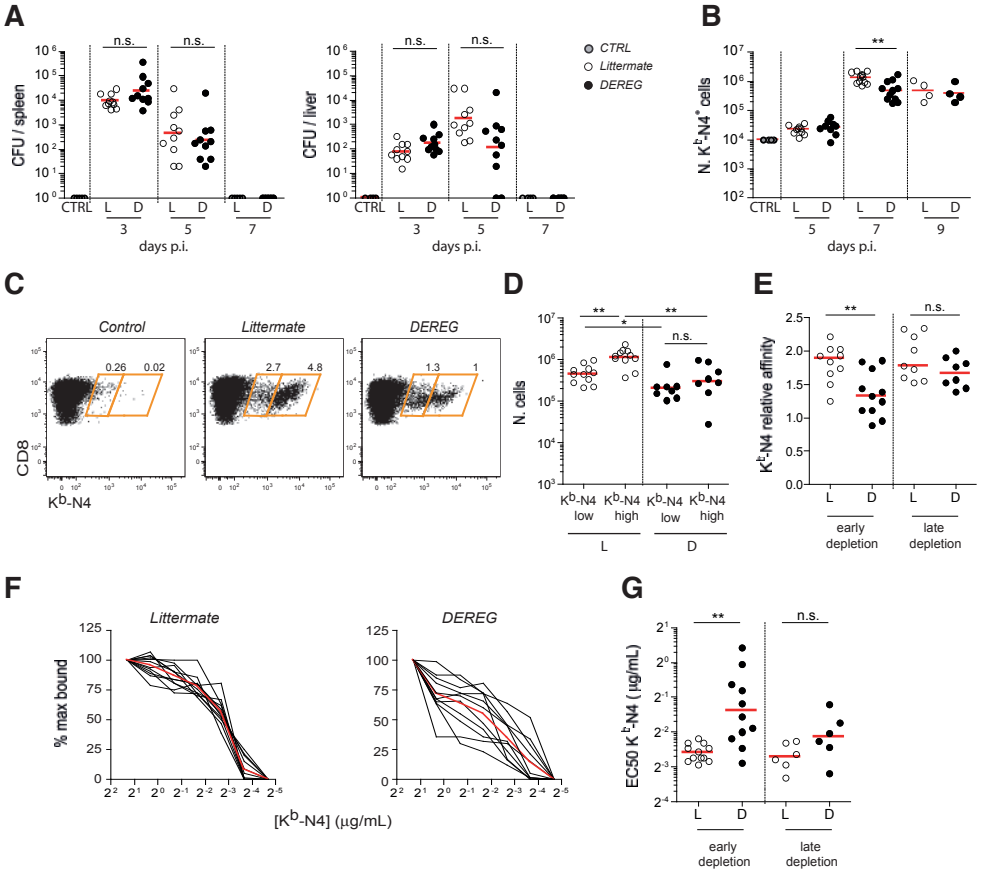

# Figure 4 Pace L. et al.